Thermal weakening localizes intraplate deformation along the southern Australian continental margin

Simon P. Holford [a,*], Richard R. Hillis [b], Martin Hand [c], Mike Sandiford [d]

[a] Australian School of Petroleum & Centre for Tectonics, Resources and Exploration (TRaX), University of Adelaide, SA 5005, Australia
[b] Deep Exploration Technologies Cooperative Research Centre, c/o University of Adelaide, SA 5005, Australia
[c] Centre for Tectonics, Resources and Exploration (TRaX), University of Adelaide, SA 5005, Australia
[d] School of Earth Sciences, University of Melbourne, VIC 3010, Australia

ARTICLE INFO

ABSTRACT

The controls on seismicity and fault reactivation in stable intraplate crust located far from active plate boundaries are poorly understood. The southern Australian continental margin has been undergoing mild levels of deformation over the past ~10 Myr, manifested today by high levels of seismicity for a stable intraplate region. However, this deformation is partitioned, with zones of abundant neotectonic faults with evidence for Pliocene–Quaternary displacement, enhanced relief (up to 1–2 km) and high seismicity (numerous $M>5$ earthquakes) such as the Flinders Ranges adjoining areas of little neotectonic activity, subdued topography and low levels of seismicity such as the Murray Basin and Nullarbor Plain. Here we present a new compilation of 192 heat flow data for the southern Australian margin. Variations in heat flow correlate well with variations in neotectonic and seismic activity, with regions of deformation corresponding to elevated heat flows of up to ~90 mW m^{-2}. We propose that the southern Australian margin provides the best evidence to-date that active intraplate deformation may be localized and controlled by the thermal properties of the crust and upper mantle.

© 2011 Elsevier B.V. All rights reserved.

1. Introduction

Plate tectonics readily accounts for deformation of plate boundaries but does not satisfactorily explain deformation and seismicity of plate interiors (Stein and Liu, 2009; Stephenson et al., 2009). Various studies have identified the thermal state of the crust and upper mantle as the dominant control on intraplate lithospheric strength (Kusznir and Park, 1982; Sonder and England, 1986) but there are few examples where localized thermal weakening of the lithosphere is demonstrably responsible for localizing deformation. It has been proposed that the elevated seismicity of the New Madrid Seismic Zone (NMSZ), Missouri, which witnessed three $M>7$ earthquakes in 1811–1812, could be explained by thermal weakening based on elevated heat flow within the NMSZ (~60 mW m^{-2}) compared to background levels in the central-eastern United States (~45 mW m^{-2}) (Liu and Zoback, 1997). 1D numerical models of lithospheric strength suggest that the heat flow observed in the NMSZ is sufficient to weaken the underlying lower crust and upper mantle and focus intraplate stresses in the upper crust, thereby localizing seismicity and deformation (Liu and Zoback, 1997). However, subsequent investigations of the NMSZ have revealed a much smaller heat flow anomaly (~3 mW m^{-2}),

implying that the lithospheric strength of the NMSZ is essentially the same as that of surrounding regions (McKenna et al., 2007). NMSZ seismicity has most recently been attributed to migrating seismicity across zones of similarly reduced strength e.g. failed rifts (McKenna et al., 2007) or to reductions in upper crustal normal stresses induced by incision-driven unloading and flexure of the lithosphere (Calais et al., 2010), but the question of the extent to which intraplate deformation and reactivation may be localized by the thermal architecture of the lithosphere remains open (Sandiford and Egholm, 2008).

Whereas clear relationships between thermal weakening of the lithosphere and localized intraplate deformation have been difficult to establish, the geological record contains numerous examples of structural reactivation during episodes of intraplate orogeny and basin inversion (Holdsworth et al., 1997; Turner and Williams, 2004), leading to the viewpoint that pre-existing zones of mechanical weakness (e.g. faults, shear zones, failed rifts, and compositional boundaries) exert the first-order control on the localization of intraplate deformation (Sykes, 1978). However, relatively little attention has been paid to regions that contain structures favorably orientated for reactivation but exhibit no record of seismic/neotectonic activity.

Here we examine the controls on localized intraplate deformation along the southern Australian margin (SAM), which shows strong spatial partitioning of neotectonic and seismic activity. Through comparison with a new compilation of 192 surface heat flow

* Corresponding author.
  E-mail address: simon.holford@adelaide.edu.au (S.P. Holford).

measurements (Fig. 1), we demonstrate strong correspondence between regions of neotectonic faulting, enhanced seismicity and elevated heat flow at length-scales of 100–1000 km. We believe that while mechanical weakness may control the deformation within a region, thermal weakening of the lithosphere is the primary control on which regions are prone to deformation.

2. Active tectonics of the southern Australian margin

Australia is among the most active 'stable continental regions' (Braun et al., 2009; Célérier et al., 2005; Leonard, 2008; Sandiford, 2003) with a seismic moment release rate of order 10^{-17}–10^{-16} s^{-1}, several times higher than comparable intraplate regions (e.g. Europe and Africa) (Sandiford and Egholm, 2008). Much of this seismicity occurs along the SAM, which formed following Cretaceous–Paleogene breakup with Antarctica and has markedly heterogeneous basement geology characterized by numerous Archaean–Paleozoic terranes (Teasdale et al., 2003). Present-day seismicity is partitioned into several distinct seismic zones separated by regions with considerably fewer earthquakes (Leonard, 2008). Most contemporary seismic activity in south-central Australia occurs in the Flinders seismic zone (FSZ) (Fig. 1) which corresponds with the topographically elevated Flinders and Mt Lofty Ranges, and the eastern Eyre Peninsula, where earthquakes as large as M_S ~6 have been recorded (Fig. 2). There is also a ~SW–NE trending region of elevated seismicity termed the southeast seismic zone (SESZ) that largely overlaps with the elevated topography of the Southeastern Highlands. Between the FSZ and the SESZ is an area of markedly reduced earthquake activity corresponding to the Murray Basin. To the west of the FSZ, the number of recorded earthquakes dramatically reduces in the Eucla and Bight basins, but increases in the Yilgarn Craton west of ~128°E.

The distribution of seismicity shows remarkable correspondence with the neotectonic record of the SAM (Fig. 1). The Flinders and Mt Lofty Ranges have been undergoing uplift due to ~E–W shortening over the past 10 Myr (Célérier et al., 2005), and palaeoseismic studies of Quaternary faults that bound the ranges have estimated slip rates of 20–100 m Myr^{-1} and maximum magnitude earthquake events of M_W ~7.3 (Quigley et al., 2006). In SE Australia, Miocene and older sediments have been deformed by folding and reverse faulting induced by approximately NW–SE crustal shortening from the late Miocene onwards (Holford et al., 2011; Sandiford, 2003). Shuttle Radar Topography Mission (SRTM) images of the Southeastern Highlands reveal numerous NNE and ENE-trending faults, along

which reverse movements of up to several hundred metres have contributed to Pliocene-onwards uplift (Holdgate et al., 2008).

In contrast, there are relatively few compressional structures in the topographically subdued and seismically quiet Murray Basin (Sandiford, 2003), onshore Eucla Basin and offshore Bight Basin where seismicity levels are among the lowest of any part of the continent (Hillis et al., 2008). The EB contains the Nullarbor Plain, a marine limestone terrace >1000 km long that was exposed ~15 Myr ago by long-wavelength uplift of the SAM (Sandiford, 2007). SRTM images across the Nullarbor Plain reveal a number of linear north–south trending faults, but maximum displacements on these structures are generally ~10 m, considerably lower than inferred for faults bounding the Flinders and Mt Lofty Ranges (Hillis et al., 2008).

The orientations of compressional neotectonic structures along the SAM are generally consistent with an E–W to SE–NW orientated S_{Hmax} controlled by plate boundary forces (Hillis et al., 2008; Reynolds et al., 2002; Sandiford et al., 2004). Basement structure maps of the southern margin indicate a high degree of mechanical anisotropy in the upper crust, and show numerous NE–SW and N–S trending structures in the Murray, Eucla and Bight basins that should be suitably oriented for failure in the *in situ* stress field (Teasdale et al., 2003). The paucity of neotectonic structures and low levels of seismicity in these regions imply an additional control on localization of deformation. Recent numerical modeling suggests that rheological contrasts between geological provinces and evolving plate boundary forces could explain strain localization (Dyksterhuis and Müller, 2008), but other workers (e.g. Célérier et al., 2005) have noted a correlation between the spatial extents of the FSZ and the South Australian heat flow anomaly, a zone of elevated heat surface flow (average 92 ± 10 mW m^{-2}) (Neumann et al., 2000), and thus attributed active intraplate deformation to thermal weakening.

3. Present-day heat flow and distribution of intraplate deformation

We have compiled a new map of the surface heat flow of the SAM, based on 192 measurements comprising published data (e.g. Cull, 1982; Goutorbe et al., 2008; Fig. 1) and recently reported estimates from geothermal exploration (Supplementary Table 1). Data density is greatest in regions of resource exploration (e.g. Flinders Ranges and Otway Basin). Measurements are sparser in the Eucla and Bight basins, but the quality of these estimates is generally good (Cull, 1982). Small-scale heat flow anomalies can result from groundwater
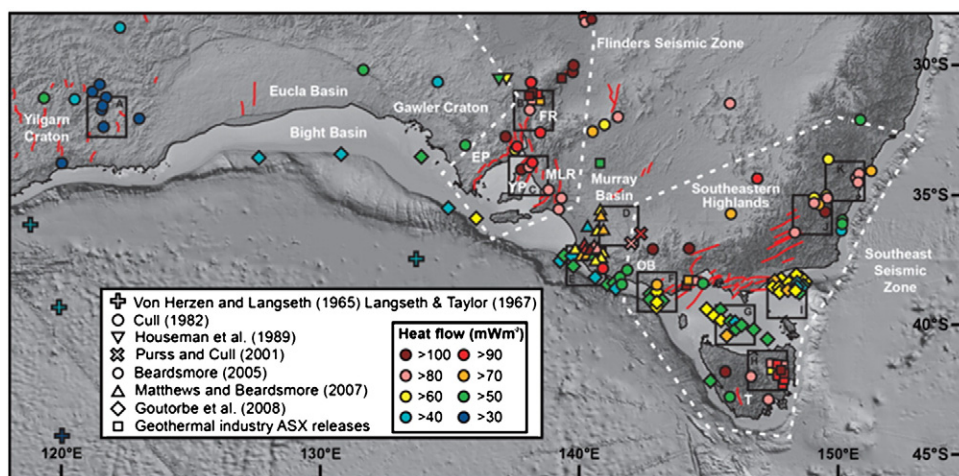
Fig. 1. Heat flow and neotectonics of the southern Australian margin. Note localization of neotectonic fault scarps (red) in regions such as the Flinders/Mt Lofty Ranges and Southeastern Highlands (Hillis et al., 2008; Holdgate et al., 2008; Holford et al., 2011), relatively few structures in the Murray and Eucla basins, and the correspondence of the distribution of faults with the Flinders and Southeast seismic zones (Leonard, 2008). Full details of references used to compile heat flow database provided in Supplementary Information. Map also shows the positions of 1.5 × 1.5 cells used to compare heat flow and seismic energy release in Fig. 4B. EP, Eyre Peninsula; FR, Flinders Ranges; MLR, Mt Lofty Ranges; OB, Otway Basin; YP, Yorke Peninsula.
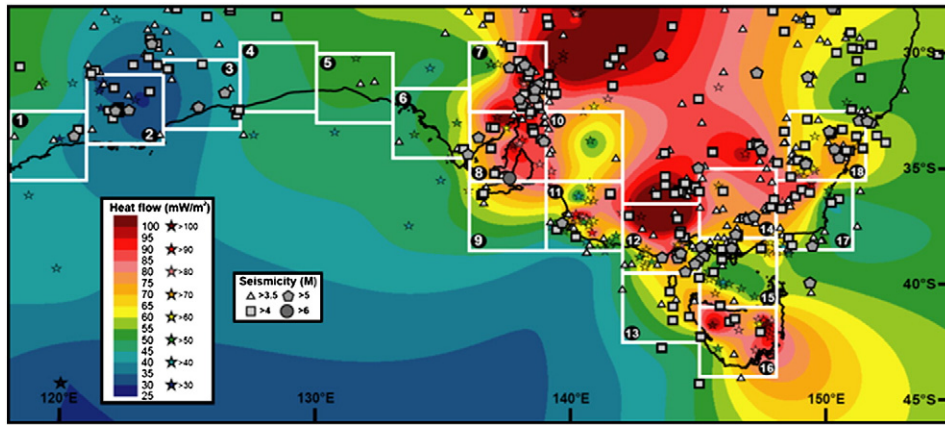
Fig. 2. Contoured (kriged) heat flow map with superimposed seismicity, demonstrating strong qualitative correlation between regions of high levels of heat flow and elevated seismicity, particularly along the southeastern margin. Map also shows the 3°×3° cells used in the quantitative comparison of heat flow and seismicity (Fig. 4A).

flow (McKenna et al., 2007), which contributes to elevated geothermal gradients observed in parts of central Australia, but the majority of measurements from the SAM are thought to reflect crustal properties (Neumann et al., 2000). We note that the number of reliable heat flow measurements available for the SAM is low in comparison to those available with other continental regions of comparable size such as western North America and northwest Europe (Pollack et al., 1993).

Our map provides better definition of individual heat flow provinces than previous studies (e.g. Cull, 1982) (Fig. 2). Heat flow increases from west to east along the margin, from values of ~35–40 mW m^{-2} at longitudes <125°E to mostly >80 mW m^{-2} between 135 and 150°E, but some notable short-wavelength variations are superimposed on this regional pattern. Heat flow locally exceeds >100 mW m^{-2} in the Flinders Ranges, Tasmania and western parts of the southeastern Highlands. There are noticeable reductions in heat flow within the Murray, Eucla and Bight basins with reported values >30 mW m^{-2} lower than adjacent regions.

The spatial variation of heat flow and that of neotectonic structures and/or seismicity generally show clear correspondence (Figs. 1, 2). Regions of high heat flow such as the Flinders Ranges and Southeastern Highlands are characterized by relatively high seismicity, while the Murray, Bight and Eucla basins experience few earthquakes and contain few neotectonic faults. SRTM images of the Eyre Peninsula–Flinders/Mt Lofty Ranges illustrate these associations well (Fig. 3). The Flinders and Mt Lofty Ranges, Yorke Peninsula and
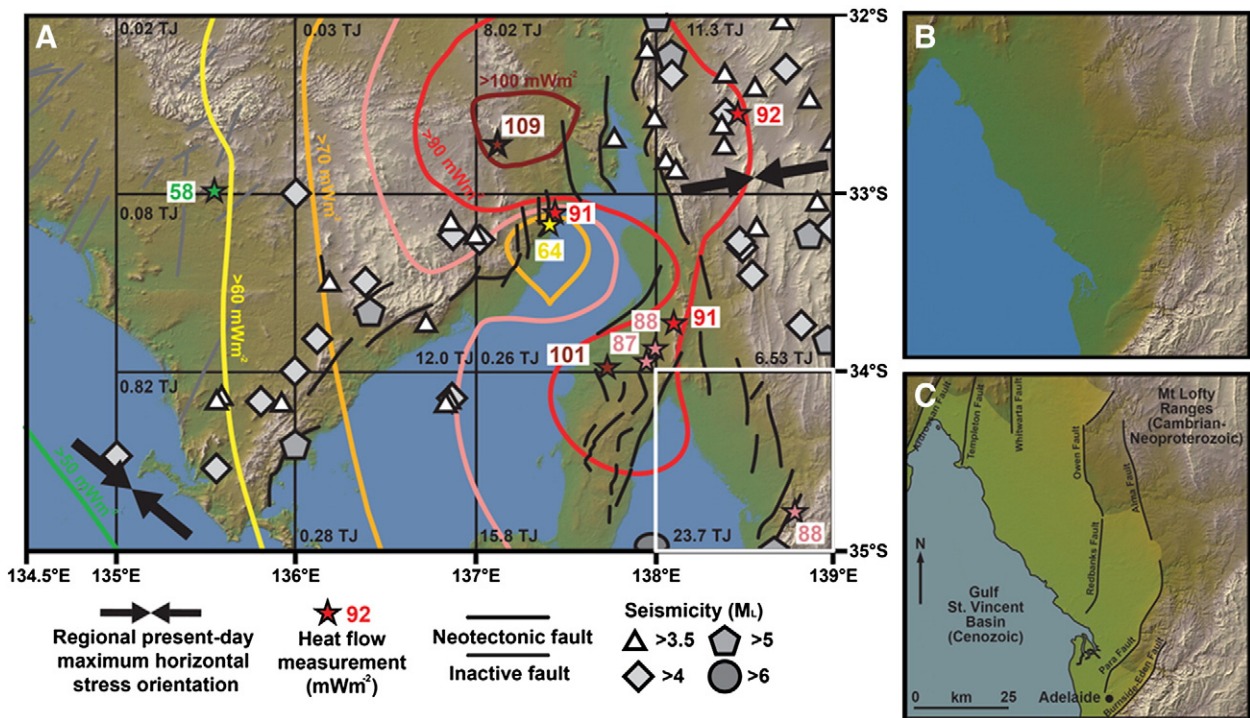
Fig. 3. (A) STRM 3 arcsecond image of area encompassing the southwestern Flinders and Mt Lofty Ranges and Eyre Peninsula, with superimposed heat flow, seismicity, regional S$_{Hmax}$ orientations (Hillis et al., 2008) and neotectonic fault scarps identified through interpretation of STRM data. Note density of faults (black) along the western Mt Lofty and Flinders Ranges, Yorke Peninsula and eastern Eyre Peninsula. There is a clear decrease in neotectonic structures and seismicity as heat flow decreases towards the central and western Eyre Peninsula. Grey features are faults identified from 1:250,000 geological maps that are favorably oriented for reactivation under present-day stress conditions but have no distinct topographic expression and thus inferred to be inactive. Seismic energy release is calculated for twelve 1°×1° cells and again there is a strong spatial correlation between seismic energy release and heat flow. (B) Uninterpreted STRM image of Mt Lofty Ranges east and north of Adelaide, South Australia, illustrating high quality of data used to identify neotectonic faults. (C) Interpreted image highlighting neotectonic faults that bound Mt Lofty Ranges and Yorke Peninsula and displace Eocene–Holocene sediments of the Gulf St Vincent basin.

eastern Eyre Peninsula, where the present-day heat flow field is best defined due to a relatively high density of measurements that define a clear, well constrained zone of elevated heat flow (>80 mW m^{-2}) are flanked by numerous faults that displace Pliocene–Quaternary rocks (Quigley et al., 2006; Sandiford, 2003) and have witnessed frequent M>5 earthquakes. In the western and northern Eyre Peninsula (heat flow <60 mW m^{-2}) there is little recorded seismicity or neotectonic faulting, despite this region containing numerous NE–SW basement structures that are favorably oriented for reactivation under the prevailing NW–SE to W–E S_{Hmax}.

While there is an evident association between high heat flow and neotectonic structures/present-day seismicity based on available data in areas such as the Flinders Ranges and Southeastern Highlands, there are also several parts of the SAM where the association between heat flow and faulting is less clear. For example, there is little historical seismicity in eastern Tasmania (Fig. 2) despite a number of reported heat flow measurements of >90 mW m^{-2}. In contrast, there are many earthquakes in western parts of the SAM, where reported heat flows are among the lowest across Australia (Cull, 1982).

To evaluate the potential relationship between surface heat flow and the deformation of the SAM, we compared average heat flow with the amount of seismic energy released by earthquake activity in eighteen 3°×3° cells. The configuration of these cells broadly mimics the main physiographic elements of the margin. We utilized a comprehensive catalogue of Australian earthquakes between 1900 and 2007 (Leonard, 2008). The earthquakes used in our study meet the rigorous catalogue completeness cut-off levels that have been determined for Australia by Leonard (2008). After screening to remove aftershocks and duplicates following the methods of Braun et al. (2009) (Supplementary Methods), we estimated the amount of seismic energy released in each cell using an empirical relationship that relates seismic energy to earthquake magnitude:

$$\log E_S = 1.5 M_S + 4.8 \tag{1}$$

where E_S is the radiated seismic energy (Joules) and M_S is the measured surface wave magnitude (Scholz, 2002).

Fig. 4A compares total seismic energy (TJ) with average heat flow (Q; calculated using the smoothed grid presented in Fig. 2) for the eighteen cells. There is a clear positive correlation between heat flow and seismic energy. The six cells that exhibit the greatest seismic energy release (>50 TJ) are in the FSZ and SESZ. In cells that cover the quiescent Bight and Eucla basins, Q is ~48–55 mW m^{-2} and E_S is ~1–4 TJ. There are two major exceptions to the positive correlation between Q and E_S. Cells in the western part of the margin exhibit unusually high levels of seismic activity at heat flow values of ~35–42 mW m^{-2}. This elevated seismicity, much of which occurs at depths <5 km (Leonard, 2008), may be linked to the anomalously high horizontal stress magnitudes at shallow upper crustal depths that have been inferred from overcoring tests in hard rock mines (Lee et al., 2006). These indicate that maximum principal horizontal stress magnitudes at 1 km depth in the Yilgarn Craton are approximately double those observed at equivalent depths in hard rock mines elsewhere in Australia (Lee et al., 2006). In cell 10 covering the Murray Basin, Q is ~73 mW m^{-2} but E_S is only ~1 TJ (the high heat flow may be due to the cell 'capturing' some of the elevated heat flow in the FSZ and SESZ). Excluding the MB and western cells, a linear regression yields a statistically significant correlation coefficient (r) of 0.8 between Q and E_S (coefficient of determination (R^2) = 0.64, two-tailed p-value = 0.0006). To demonstrate that a consistent relationship between heat flow and seismicity exists at a variety of spatial scales, in Fig. 3A we estimate the amount of seismic energy release in twelve 1°×1° cells that cover the transition from the Eyre Peninsula to the FSZ. There is a clear increase in E_S from <1 TJ in cells that cover the western Eyre Peninsula, where measured heat flows are <60 mW m^{-2}, to >5–20 TJ in cells that cover the FSZ, where heat flows reach >90 mW m^{-2}.
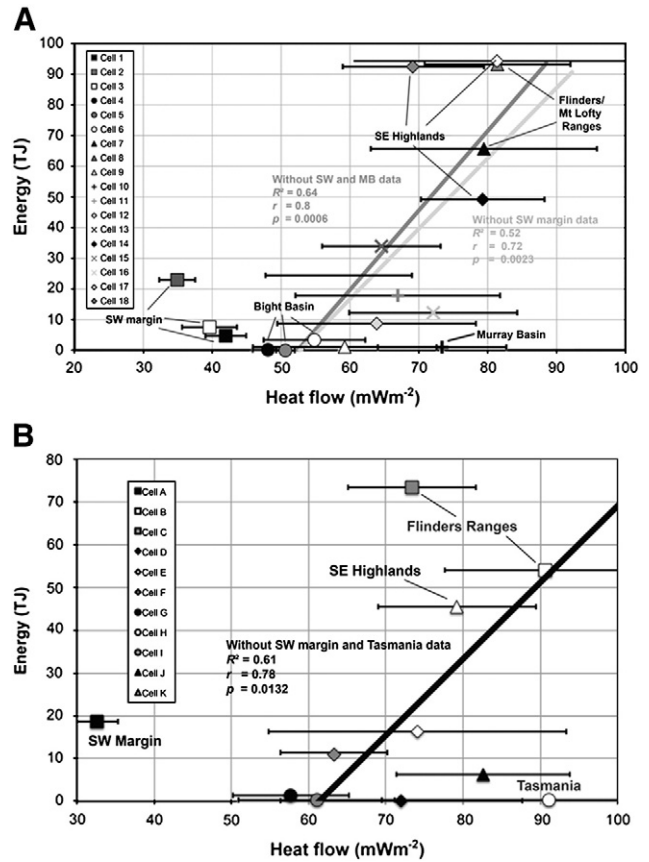

Fig. 4. (A) Comparison of average heat flow (mW m^{-2}) and absolute seismic energy release (TJ) for the eighteen 3°×3° cells. Average heat flow calculated by averaging values from the kriged grid at 30 minute intervals. Seismic energy calculated from earthquakes in each cell that meet catalogue completeness levels (Supplementary Information). (B) Comparison of average heat flow and absolute seismic energy release for 1.5°×1.5° cells that contain ≥5 heat flow measurements.

We consider the observed correlations a surprisingly good result considering: the wide range of factors that may potentially influence intraplate seismicity (e.g. Stein, 2007); our poor understanding of the relative accommodation of strain by seismic and aseismic mechanisms (Célérier et al., 2005); and, that the ~100 year record of historical seismicity for the SAM is up to several orders of magnitude shorter than recurrence intervals calculated for large (e.g. M>6) earthquakes in this region (~10^4 to 10^5 years; Crone et al., 2003; Quigley et al., 2006). Given the logarithmic nature of seismic energy release, it is necessary to consider how the presence or absence of such large earthquakes may affect our results. Fig. 5 shows a Gutenberg–Richter relationship ($\log N = a - bM$) (Gutenberg and Richter, 1944) determined for the SAM using the earthquakes we used to calculate seismic energy release. This relationship yields a and b values of 5.35 and 0.78 respectively, with a robust least squares R^2 value of 0.95. Though the estimate of a is consistent with values of 5.2–5.4 calculated for the FSZ and SESZ by Leonard (2008), the somewhat lower value of b is probably influenced by the unusual seismic record of the western SAM, where Leonard (2008) estimated a value of 0.58 for b, which is low by world standards. Our estimate of b is also impacted by the removal of many small (i.e. M<2) earthquakes that did not meet the catalogue completeness levels defined by Leonard (2008), though the comparatively small amount of seismic energy released during these events means that our estimates of seismic energy release along the SAM are largely unaffected by their exclusion. Fig. 5 implies that more M=5–6 and fewer M>6 earthquakes than expected occurred between 1900 and 2007,
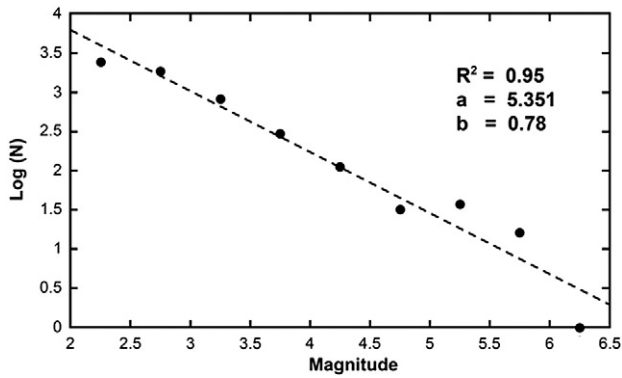
Fig. 5. Gutenberg–Richter relations for the period 1900–2007 for the earthquakes used to calculate seismic energy release for the SAM.

consistent with the notion that much of Australia's ongoing seismicity might be episodic rather than temporally and spatially stationary, as advocated by Leonard (2008). However, Gutenberg–Richter relations we have derived for individual cells indicate that only those cells where observed seismic energy release is >35 TJ (and average heat flow >65 mW m^{-2}) were expected to have more than one M>6 earthquake over the time interval considered in our study. We thus consider our estimates of observed seismic energy release to be reasonably representative of the expected energy release, and that the absence of some anticipated large events has not overtly affected the relationship between heat flow and seismicity we have described. Most importantly, the strong coherence between parts of the SAM that demonstrate highest seismic energy release and the distribution of recognised neotectonic faults (Figs. 1–3) lend strong credence to the notion that the ~10^2 year record of deformation inferred from seismicity is broadly representative of the longer term (~10^6–10^7 years) record of deformation witnessed by neotectonic faulting.

Although the correlation between heat flow and seismicity demonstrated in Fig. 4A is supported by the neotectonic faulting record, the relatively low density of heat flow measurements across some parts of the SAM raises the possibility that the correlation may be influenced by spatial aliasing in cells that contain few heat flow data. To address this possibility we imposed a grid of 1.5°×1.5° cells upon the SAM and calculated the absolute seismic energy release and average heat flow for all cells that contained ≥5 heat flow measurements (Fig. 1A). In total, eleven cells met this criterion, ten of which were located east of 137°30′E, reflecting the higher density of heat flow measurements acquired in the eastern SAM. The results of our analysis are displayed in Fig. 4B, which replicates many of the features of the analysis based on the coarser 3°×3° cell size (Fig. 4A). The main exceptions to the positive correlation between heat flow and seismic energy release are cell A from the western SAM which, as discussed earlier, demonstrates moderate seismic activity ($E_S \approx 19$ TJ) and very low heat flow (~33 mW m^{-2}), and cell H, which covers eastern Tasmania. The thirteen heat flow measurements within cell H define an average value of ~91 mW m^{-2}, (most likely related to buried granites) but seismic energy release is <1 TJ (Fig. 4B). Eastern Tasmania clearly departs from the positive correlation between heat flow and seismic energy release, though high heat flows (i.e. ~91 ± 22 mW m^{-2}) are recorded by the few measurements obtained in western Tasmania (Fig. 1), where historical seismicity is higher than across eastern Tasmania (Fig. 2) and both neotectonic uplift (Murray-Wallace and Goede, 1995) and faulting (Clark et al., 2011) have been reported. Excluding the cells from the western SAM and eastern Tasmania, a linear regression yields a statistically significant correlation coefficient (r) of 0.78 between Q and E_S (coefficient of determination (R^2) = 0.61, two-tailed p-value = 0.0132). Though the

acquisition of more heat flow data across the SAM is clearly desirable to better define the spatial variation of heat flow and its relationship with seismicity, we conclude that both available data and our analyses of 3°×3° and 1.5°×1.5° cells support a relationship between elevated heat flow and active deformation of the SAM.

4. Discussion

Our observations imply that at length-scales of 100–1000 km along the SAM, thermal weakening of the lithosphere controls the location of active intraplate deformation. High heat flow in the Flinders Ranges is known to be the result of an unusual abundance of heat producing elements (i.e. U, Th, and K) in Palaeoproterozoic–Meosoproterozoic basement, witnessed by heat production rates that reach >10 μW m^{-3} (Neumann et al., 2000). The ~30 mW m^{-2} difference in heat flow between the Flinders Ranges and surrounding regions (e.g. Murray Basin and Eyre Peninsula) resulting from the burial of basement enriched in heat producing elements to depths >5 km implies that Moho temperatures could be ~90–120 °C hotter beneath the former (depending on the length-scale of the thermal anomaly), sufficiently high to reduce bulk lithosphere strength by a factor of 2–5 and focus deformation (Célérier et al., 2005).

Shear wavespeeds at 100 km depth beneath the Bight, Eucla and Murray basins are ~5% faster than beneath the FSZ and SESZ (Fishwick et al., 2008), which implies that the lithosphere at 100 km beneath the deforming regions may be >100 °C hotter (Goes et al., 2005). Numerical modelling indicates that Moho temperature variations as small as 10–30 °C may explain the elevated levels of seismicity observed along southwestern parts of margin, due to steady-state heat flow across the oceanic-continental lithospheric step (Sandiford and Egholm, 2008). The observation that the seismicity of the SESZ broadly parallels the architecture of the continental margin and crosscuts underlying structural trends (Teasdale et al., 2003) suggests that lateral heat flow may also play a role in localizing that deformation.

Here we present a model that relates thermal weakening to the intensity of fault reactivation along the SAM (Fig. 6). Regions characterized by elevated heat flows (e.g. FSZ and SESZ) are underlain by anomalously high Moho temperatures that may be due to enhanced mantle heat flux, a crust enriched with heat producing elements, or a combination of both these factors. Thermally activated creep dissipates stresses in the ductile lower crust and upper mantle, causing significant stress amplification in the brittle upper crust (Kusznir and Park, 1986), where failure is most likely to occur by reshear of pre-existing faults that are favorably oriented for reactivation (Sibson, 1995), with some degree of spatial migration between different fault systems likely (Li et al., 2011). In regions characterized by normal or reduced heat flows (e.g. Eucla Basin), stresses are distributed more uniformly throughout the lithosphere with less amplification in the brittle upper crust, where fault reactivation is consequently less pervasive and slip rates are accordingly lower. Our model is consistent with histograms of earthquake depths in the FSZ and SESZ, which show peaks at depths of ~10–12 km (e.g. Leonard, 2008).

4.1. Alternative causes of elevated heat flow and seismicity

Here we consider the other factors that may influence the observed seismicity and heat flow. First we address the possibility that the zones of elevated heat flow are in fact caused by seismic activity. Radiogenic decay is by far the most important mechanism of heat generation within the crust, but other sources can affect surface heat flow in localised regions, including frictional heating from faulting (Beardsmore and Cull, 2001). This occurs when work done in overcoming friction dissipates into the surrounding rock as heat. The frictional heat (Q_f) generated by a slow-creeping fault is proportional
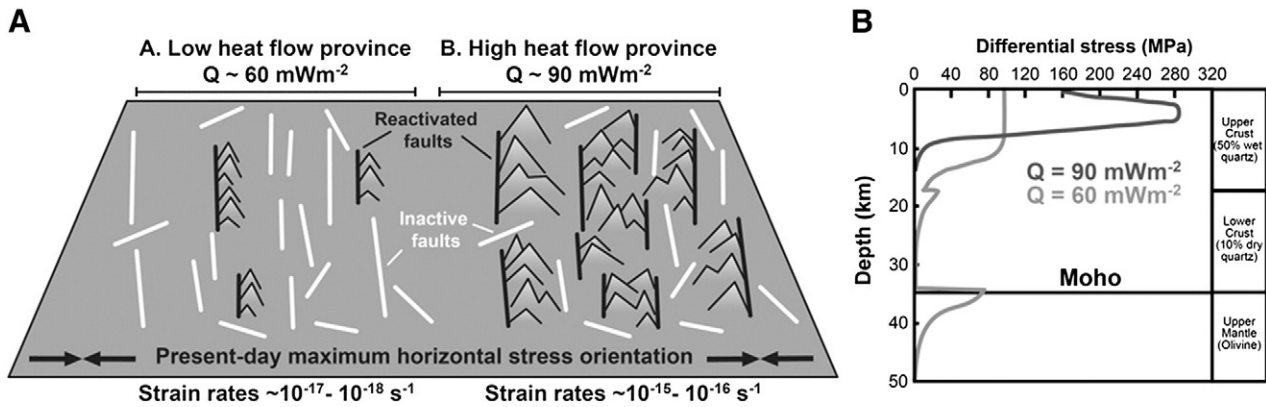
Fig. 6. Model for thermally-controlled intraplate fault reactivation. (A) Schematic perspective view map of region of intraplate region characterized by two provinces of low (~60 mW m^{-2}) and high (~90 mW m^{-2}) heat flow, analogous to the Eucla Basin and Flinders/Mt Lofty Ranges of the SAM. Present-day maximum horizontal stress orientations are known for both provinces, which each province contains numerous pre-existing faults of varying planform orientations all of which dip at 30°. In the low heat flow province relatively few faults have been reactivated, and many faults that are suitably oriented for reactivation under the prevailing stress regime are inactive. This contrasts with the high heat flow province where a much higher proportion of suitably oriented faults have been reactivated. Faults in the high heat flow province that remain inactive despite being favorably oriented for reactivation may have higher coefficients of friction. Strain rates in the high heat flow province are correspondingly higher than in the low heat flow province. (B) Stress–depth plots for column of intraplate lithosphere 100 km thick that has been subjected to a compressional force of ~1.9×10^{12} N m^{-1} for 1 Myr with geothermal gradients that correspond to surface heat flow values of 60 and 90 mW m^{-2} similar to those that characterize the low and high heat flow provinces in A (modified after Kusznir and Park, 1986). At high heat flow values, stresses in the lower crust are dissipated by thermally activated creep resulting in significant stress amplification in the brittle upper crust in comparison to low heat flow values. The enhanced stress magnitudes in the brittle upper crust at high heat flow values result in more pervasive reactivation of pre-existing faults that are favorably oriented for reshear under the present-day stress regime.

to the distance from the top to the bottom of the fault (d), the velocity or slip rate of the fault (u) and the shear stress acting on the fault (τ):

$$Q_f = d \times u \times \tau. \tag{2}$$

This implies that a fault is only likely to exert a significant effect on nearby surface heat flow if either the slip rate or shear stress is high (i.e. $u > 10$ cm yr^{-1} or $\tau > 20$ MPa) (Beardsmore and Cull, 2001). Low long-term (>1 Myr) slip rates are estimated in the Flinders Ranges ($u \approx 0.002$–0.015 cm yr^{-1}) (Sandiford, 2003) which implies that shear stresses would need to be unreasonably large for frictional heating from faulting to contribute appreciably to the observed surface heat flows. Consequently we rule out any contribution from seismicity itself to the observed surface heat flows in our study area. Indeed the relationship between high heat production and high heat flow in the Flinders Ranges suggests that high heat flow is not caused by frictional heating.

Secondly we consider the likelihood that variations in crustal structure may exert the primary control on the distribution of seismicity. Many regions of concentrated intraplate seismic activity are spatially associated with failed rifts (Schulte and Mooney, 2005) where the crust may be relatively thin and weak compared to surrounding regions. Comparisons of maps of Australian seismicity (Fig. 2) and crustal thicknesses (Collins et al., 2003) (Fig. 7A) display few similarities that would suggest that crustal structure imposes an overriding control on the distribution of deformation. For example, crustal thickness patterns in the FSZ are similar to those in the western Eyre Peninsula, where seismicity is much lower. The MB is underlain by crust that is >5 km thinner than the adjacent FSZ and SESZ, but is characterized by considerably fewer earthquakes. Crustal thicknesses beneath the SESZ range from ~30 to 50 km, indicating no obvious relationship with seismicity. It is also notable that the SESZ crosscuts the predominant N–S structural grain of the Lachlan Orogeny (Fig. 7B), which separates provinces with distinct rock types and structural–metamorphic histories (Foster and Gray, 2000). These observations imply that crustal structure does not control the distribution of seismicity to first-order.

Finally, we evaluate the possibility that the distribution of seismicity is related to pre-existing topographic gradients. It has

been suggested that a large proportion of Australian seismicity might result from post-tectonic isostatic rebound of regions that were elevated during earlier tectonic events (Lambeck et al., 1989). However, most earthquakes in the FSZ and SESZ reveal compressional and oblique-slip focal mechanisms (Clark and Leonard, 2003), rather than normal faulting which might be expected if isostatic rebound of topographically elevated regions was the primary factor controlling seismicity (Braun et al., 2009).

4.2. Thermal controls on the frequency and extent of intraplate deformation and fault reactivation

As in many intraplate settings, factors such as pre-existing structural weaknesses and zones of overpressured crust probably play an important role in the distribution of deformation (Holdsworth et al., 1997; Sibson, 1995; Turner and Williams, 2004). However, we believe that the potential for localization of deformation by the thermal architecture of the crust and lithosphere is often overlooked, especially at the terrane scale, because reactivation of pre-existing zones of structural weakness is preferentially invoked. There is growing support for the thermal properties of the crust exerting a first-order control on focussing intraplate deformation from studies around the world. In a passive continental margin setting analogous to the SAM, post-rift compressional structures are common in the Cretaceous–Cenozoic Vøring Basin but are rarely observed in the adjacent Triassic–Jurassic Halten Terrace along the Norwegian Atlantic margin (Doré et al., 2008). This pattern of intraplate deformation is attributed to the presence of thinner, hotter and weaker basement beneath the Vøring Basin (Doré et al., 2008). Intraplate deformation in cold lithosphere (~45 mW m^{-2}) in southeastern Ukraine preferentially occurs in the >20 km thick Dniepr–Donets Basin as a consequence of thermal refraction stemming from bulk thermal conductivity in the sedimentary basin that is lower than adjacent crystalline basement (Stephenson et al., 2009). In Central Australia it is postulated that spatial and temporal variation in thermal weakening of the lithosphere due to shifting subsidence patterns exerted a modulating effect on the pattern of basement fault reactivation during intraplate orogeny (Hand and Sandiford, 1999).
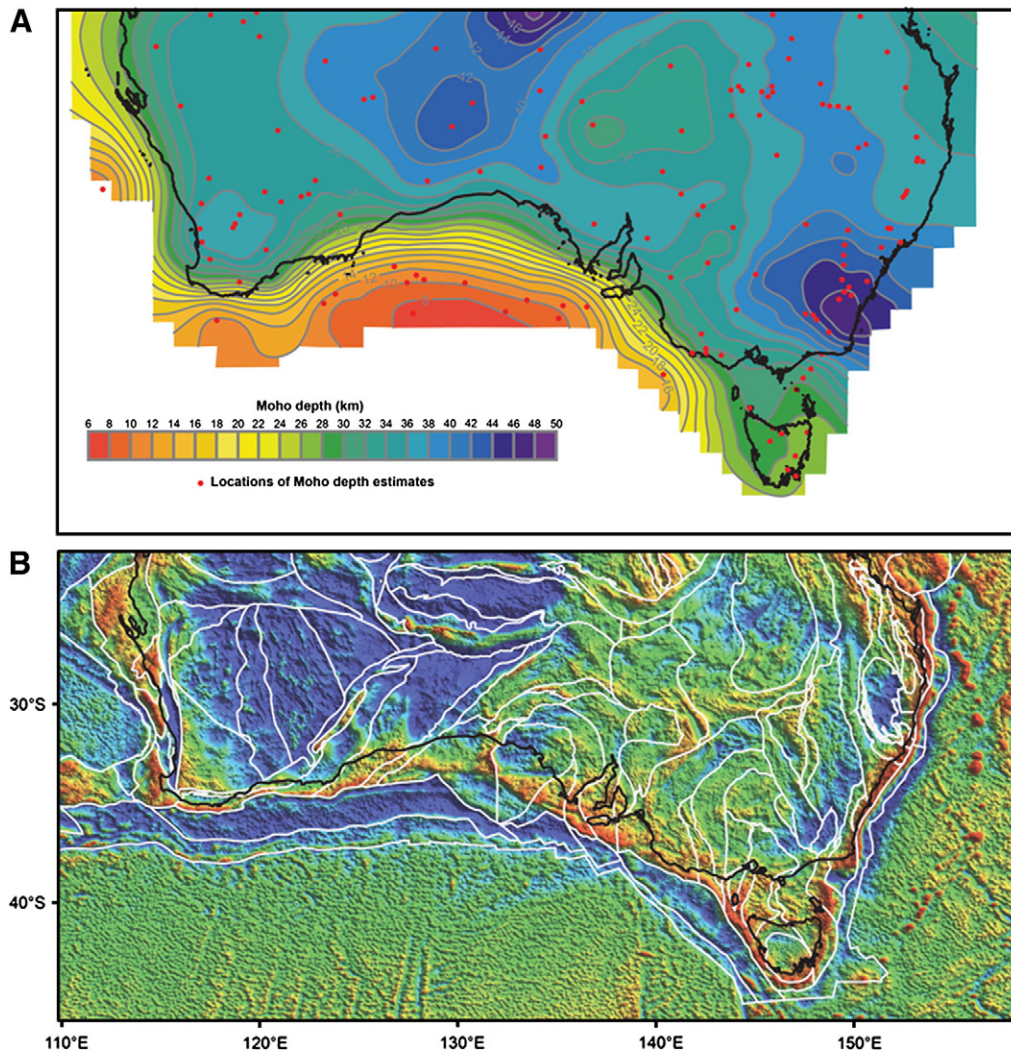
Fig. 7. Crustal thickness, gravity anomalies and basement structure of the southern Australian margin. (A) Seismologically determined crustal thickness map for the SAM (Modified after Collins et al., 2003). Comparison with Figs. 1 and 2 indicates little obvious correspondence between variations in crustal thickness and the distribution of elevated heat flow or seismicity. (B) Gravity map (onshore, Bouger corrected; offshore, free-air) of the SAM with basement terranes (structurally-bound regions with common depositional, deformational, volcanic and metamorphic histories) superimposed (FrOG Tech Pty Ltd, 2005). Again comparison with Figs. 1 and 2 reveals little few clear correlations between zones of elevated seismicity heat flow and significant gravity (and thus crustal density) anomalies and gradients. Similarly comparison with Figs. 1 and 2 indicates that the well-defined seismic zones of the southern Australian margin largely cross-cut underlying structural boundaries, particularly in the case of the SESZ which trends approximately ~SW–NE, oblique to the underlying ~N–S structural trends imparted by the Palaeozoic Lachlan orogeny (Foster and Gray, 2000).

5. Conclusion

The distribution of neotectonic structures and present-day seismicity along the southern Australian margin shows a strong correspondence with the pattern of surface heat flow, implying that thermal weakening has localized intraplate deformation. We propose that in this, and potentially other intraplate settings, the thermal properties of the crust and upper mantle exert a regional-scale (100–1000 km) modulating control on which parts of the lithosphere undergo failure and which parts experience relatively less deformation.

More heat flow data, particularly from the western SAM are desirable to further refine our model, but our results indicate that a better understanding of the thermal structure of the crust may aid in seismic risk assessment in intraplate regions characterized by elevated levels of seismicity, e.g. India and North America (Stein and Liu, 2009).

Appendix A. Supplementary data

Supplementary data to this article can be found online at doi:10.1016/j.epsl.2011.02.056.

References

Beardsmore, G.R., Cull, J.P., 2001. Crustal Heat Flow: A Guide to Measurement and Modelling. Cambridge University Press, Cambridge.
Braun, J., Burbidge, D.R., Gesto, F.N., Sandiford, M., Gleadow, A.J.W., Kohn, B.P., Cummings, P.R., 2009. Constraints on the current rate of deformation and surface uplift of the Australian continent from a new seismic database and low-T thermochronological data. Aus. J. Earth Sci. 56, 99–110.
Calais, E., Freed, A.M., Van Arsdale, R., Stein, S., 2010. Triggering of New Madrid seismicity by late-Pleistocene erosion. Nature 466, 608–611.
Célérier, J., Sandiford, M., Hansen, D.L., Quigley, M., 2005. Modes of active intraplatedeformation, Flinders Ranges, Australia. Tectonics 24, TC6006.
Clark, D., Leonard, M., 2003. Principal stress orientations from multiple focal-plane solutions: new insight into the Australian intraplate stress field. In: Hillis, R.R.,

Müller, R.D. (Eds.), Evolution and Dynamics of the Australian Plate. Special Publication, vol. 22. Geological Society of Australia and Special Paper, Vol. 372. Geological Society of America, pp. 91–105.

Clark, D., Cupper, M., Sandiford, M., Kiernan, K., 2011. Style and timing of late Quaternary faulting on the lake Edgar Fault, southwest Tasmania, Australia: implications for hazard assessment in intracratonic areas. In: Audemard, F., Michetti, A., Macalpin, J. (Eds.), Geological Criteria for Evaluating Seismicity Revisited: 40 Years of Paleoseismic Investigations and the Natural Record of Past Earthquakes. Special Paper, Geological Society, America.

Collins, C.D.N., Drummond, B.J., Nicoll, M.G., 2003. Crustal thickness patterns in the Australian continent. In: Hillis, R.R., Müller, R.D. (Eds.), Evolution and Dynamics of the Australian Plate. Special Publication, vol. 22. Geological Society of Australia and Special Paper, Vol. 372. Geological Society of America, pp. 121–128.

Crone, A.J., de Martini, P.M., Machette, M.N., Okumura, K., Prescott, J.R., 2003. Paleoseismicity of aseismic Quaternary faults in Australia: implications for fault behaviour in stable continental regions. Bull. Seism. Soc. Am. 93, 1913–1934.

Cull, J.P., 1982. An appraisal of Australian heat-flow data. BMR J. Aus. Geol. Geophys. 7, 11–21.

Doré, A.G., Lundin, E.R., Kusznir, N.J., Pascal, C., 2008. Potential mechanisms for thegenesis of Cenozoic domal structures on the NE Atlantic margin: pros, cons and somenew ideas. In: Johnson, H., Doré, A.G., Gatliff, R.W., Holdsworth, R., Lundin, E.R., Ritchie, J.D. (Eds.), The Nature and Origin of Compression in Passive Margins. Special Publication, vol. 306. Geological Society, London, pp. 1–26.

Dyksterhuis, S., Müller, R.D., 2008. Cause and evolution of intraplate orogeny in Australia. Geology 36, 495–498.

Fishwick, S., Heintz, M., Kennett, B.L.N., Reading, A.M., Yoshizawa, K., 2008. Steps inlithospheric thickness within eastern Australia, evidence from surface waveto-mography. Tectonics 27, TC4009.

Foster, D.A., Gray, D.R., 2000. Evolution and structure of the Lachlan fold belt (orogen) of eastern Australia. Annu. Rev. Earth Planet. Sci. 28, 47–80.

FrOG Tech Pty Ltd, 2005. OZ SEEBASE™ Study. Public Domain Report to ShellDevelopment Australia.

Goes, S., Simons, F.J., Yoshizawa, K., 2005. Seismic constraints on temperature of the Australian uppermost mantle. Earth Planet. Sci. Lett. 236, 227–237.

Goutorbe, B., Lucazeau, F., Bonneville, A., 2008. Surface heat flow and the mantle contribution on the margins of Australia. Geochem. Geophys. Geosyst. 9, Q05011.

Gutenberg, B., Richter, C.F., 1944. Frequency of earthquakes in California. Bull. Seism. Soc. Am. 34, 185–188.

Hand, M., Sandiford, M., 1999. Intraplate deformation in central Australia, the link between subsidence and fault reactivation. Tectonophys. 305, 121–140.

Hillis, R.R., Sandiford, M., Reynolds, S.D., Quigley, M.C., 2008. Present-day stress, seismicity and Neogene-to-Recent tectonics of Australia's 'passive' margins: intraplate deformation controlled by plate boundary forces. In: Johnson, H., Doré, A.G., Gatliff, R.W., Holdsworth, R., Lundin, E.R., Ritchie, J.D. (Eds.), The Natureand Origin of Compression in Passive Margins. Special Publication, vol. 306. Geological Society, London, pp. 71–90.

Holdgate, G.R., Wallace, M.W., Gallagher, S.J., Wagstaff, B.E., Moore, D., 2008. No mountains to snow on: major post-Eocene uplift of the East Victoria highlands; evidence from Cenozoic deposits. Aus. J. Earth Sci. 55, 211–234.

Holdsworth, R.E., Butler, C.A., Roberts, A.M., 1997. The recognition of reactivation during continental deformation. J. Geol. Soc. Lond. 154, 73–78.

Holford, S.P., Hillis, R.R., Duddy, I.R., Green, P.F., Tassone, D.R., Stoker, M.S., 2011. Paleothermal and seismic constraints on late Miocene–Pliocene uplift and deformation in the Torquay sub-basin, southern Australian margin. Aust. J. Earth Sci. 58.

Kusznir, N.J., Park, R.G., 1982. Intraplate lithosphere strength and heat flow. Nature 299, 540–542.

Kusznir, N.J., Park, R.G., 1986. Continental lithosphere strength: the critical rols of lower crustal deformation. In: Dawson, J.B., Carswell, D.A., Hall, J., Wedepohl, K.H. (Eds.), The Nature of the Lower Continental Crust: Geological Society Special Publication, vol. 24, pp. 79–93.

Lambeck, K., McQueen, H.W., Stephenson, R., Denham, D., 1989. The state of stress within the Australian continent. Advan. Geophys. 2, 723–742.

Lee, M.F., Mollison, J.J., Mikula, P., Pascoe, M., 2006. In-situ rock stress measurements in western Australia's Yilgarn Craton. In: Lu, M., Li, C.C., Kjørholt, H., Dahle, H. (Eds.),

In-Situ Rock Stress: Measurement, Interpretation and Application. Proc. Int. Symp. In-situ. Rock Stress, pp. 35–42.

Leonard, M., 2008. One hundred years of earthquake recording in Australia. Bull. Seism. Soc. Am. 98, 1458–1470.

Li, M., Stein, S., Wang, H., 2011. 2000 years of migrating earthquakes in North China: how earthquakes in midcontinents differ from those at plate boundaries. Lithosphere. doi:10.1130/L129.1.

Liu, L., Zoback, M.D., 1997. Lithospheric strength and intraplate seismicity in the New Madrid seismic zone. Tectonics 16, 585–595.

McKenna, J., Stein, S., Stein, C.A., 2007. Is the New Madrid seismic zone hotter and weaker than its surroundings? In: Stein, S., Mazzotti, S. (Eds.), Continental Intraplate Earthquakes: Science, Hazard, and Policy Issues. Special Paper, vol. 425. Geological Society, America, pp. 167–175.

Murray-Wallace, C.V., Goede, A., 1995. Aminostratigraphy and electron spin resonance dating of Quaternary coastal neotectonism in Tasmania and the Bass Strait islands. Aust. J. Earth. Sci. 42, 51–67.

Neumann, N., Sandiford, M., Foden, J., 2000. Regional geochemistry and continental heat flow: implications for the origin of the South Australian heat flow anomaly. Earth Planet. Sci. Lett. 183, 107–120.

Pollack, H.N., Hurter, S.J., Johnson, J.R., 1993. Heat flow from the earth's interior: analysis of the global data set. Rev. Geophys. 31, 267–280.

Quigley, M.C., Cupper, M.L., Sandiford, M., 2006. Quaternary faults of south-central Australia: palaeoseismicity, slip rates and origin. Aus. J. Earth Sci. 53, 285–301.

Reynolds, S.D., Coblentz, D.D., Hillis, R.R., 2002. Tectonic forces controlling the regional intraplate stress field in continental Australia: results from new finite element modelling. J. Geophys. Res. 107, 2131.

Sandiford, M., 2003. Neotectonics of southeastern Australia: linking the Quaternary faulting record with seismicity and in situ stress. In: Hillis, R.R., Müller, R.D. (Eds.), Evolution and Dynamics of the Australian Plate. Special Publication, Vol. 22. Geological Society of Australia and Special Paper, Vol. 372. Geological Society ofAmerica, pp. 107–120.

Sandiford, M., 2007. The tilting continent: a new constraint on the dynamic topographic field from Australia. Earth Planet. Sci. Lett. 261, 152–163.

Sandiford, M., Egholm, D.L., 2008. Enhanced intraplate seismicity across continental margins: some causes and consequences. Tectonophys. 457, 197–208.

Sandiford, M., Wallace, M., Coblentz, D., 2004. Origin of the in situ stress field in southeastern Australia. Basin Research 16, 325–338.

Scholz, C.H., 2002. The Mechanics of Earthquakes and Faulting 2nd edn. Cambridge University Press, Cambridge.

Schulte, S.M., Mooney, W.D., 2005. An updated global earthquake catalogue for stable continental regions: reassessing the correlation with ancient rifts. Geophys. J. Int. 161, 707–721.

Sibson, R.H., 1995. Selective fault reactivation during basin inversion: potential for fluid redistribution through fault-valve action. In: Buchanan, J.G., Buchanan, P.G. (Eds.), Basin Inversion: Geological Society Special Publication, vol. 88, pp. 3–21.

Sonder, L., England, P., 1986. Vertical averages of rheology of the continental lithosphere; relation to thin sheet parameters. Earth Planet. Sci. Lett. 77, 81–90.

Stein, S., 2007. Approaches to continental intraplate earthquake issues. In: Stein, S., Mazzotti, S. (Eds.), Continental Intraplate Earthquakes: Science, Hazard, and Policy Issues. Special Paper, vol. 425. Geological Society, America, pp. 1–16.

Stein, S., Liu, M., 2009. Long aftershock sequences within continents and implications for earthquake hazard assessment. Nature 462, 97–99.

Stephenson, R., Egholm, D.L., Nielsen, S.B., Stovba, S.M., 2009. Role of thermal refraction in localizing intraplate deformation in southeastern Ukraine. Nat. Geosci. 2, 290–293.

Sykes, L.R., 1978. Intraplate seismicity, reactivation of pre-existing zones of weakness, alkaline magmatism and other tectonism post-dating continental fragmentation. Rev. Geophys. 16, 621–688.

Teasdale, J.P., Pryer, L.L., Stuart-Smith, P.G., Romine, K.K., Etheridge, M.A., Loutit, T.S., Kyan, D.M., 2003. Structural framework and basin evolution of Australia's southern margin. APPEA J. 43, 13–37.

Turner, J.P., Williams, G.A., 2004. Sedimentary basin inversion and intra-plate shortening. Earth Sci. Rev. 65, 277–304.